

Received May 27, 2019, accepted June 18, 2019, date of publication July 10, 2019, date of current version July 30, 2019.

Digital Object Identifier 10.1109/ACCESS.2019.2927160

EMI Radiation Prediction and Structure Optimization of Packages by Deep Learning

HANG JIN¹, HANZHI MA¹, MARK D. BUTALA¹, EN-XIAO LIU², (Senior Member, IEEE), AND ER-PING LI¹, (Fellow, IEEE)

¹College of Information Science and Electronic Engineering, Zhejiang University–University of Illinois at Urbana–Champaign Institute, Zhejiang University, Hangzhou 310027, China

²Institute of High Performance Computing, Agency for Science Technology and Research, Singapore 138632

Corresponding author: Er-Ping Li (liep@zju.edu.cn)

This work was supported by the National Natural Science Foundation of China under Grant 61571395.

ABSTRACT With a rapid increase in operating frequency and package complexity, conventional analysis methods cannot efficiently cope with current complex electromagnetic interference (EMI) issues. In this paper, a new method built on a deep neural network (DNN) model is proposed to accurately and rapidly predict the maximum radiated electric field at 3-meters of a wire-bond ball grid array (WB-BGA) package. The key hyper-parameters of the DNN model, such as the learning rate and type of optimizers, are discussed in depth so as to attain optimal performance. Predicted radiation results by the DNN model and the results of the full-wave simulation show good agreement. Once DNN is trained, the prediction time is in the order of milliseconds and the model size is in megabytes, which can acquire the predicted radiation quickly and accurately and save storage space. Furthermore, to prevent the radiation from exceeding requirements, package structures are optimized by adjusting those parameters sensitive to radiation and disregarding insensitive parameters. The sensitivity of these WB-BGA package structural parameters to EMI radiation can be analyzed quickly based on data with different deviations generated by the trained DNN model. The sensitive parameters are adjusted according to their correlation with EMI radiation. The effectiveness and feasibility of the optimization method are verified by the WB-BGA package with two sets of different structural parameters.

INDEX TERMS Deep learning algorithm, deep neural network, electromagnetic interference, radiation prediction, sensitivity analysis, structure optimization, WB-BGA package.

I. INTRODUCTION

At present, electromagnetic interference (EMI) issues are becoming prominent in the current design process of high-speed electronic devices and systems as the operating frequency and structural complexity rapidly increase [1]–[3]. After the design tape-out and fabrication stage, the maximum radiated electric field at 3-meters of the entire device must be evaluated to determine if it can satisfy regulatory EMI requirements, such as the Federal Communications Commission (FCC) standards. Therefore, it is imperative to develop an efficient method for fast radiation prediction. In general, commercial full-wave solvers are usually adopted to calculate the radiated emission. Nevertheless when structural parameters are designed by prior experience, EMI radiation needs

to be repeatedly evaluated, which takes extremely long time without an efficient way of EMI prediction. In previous studies, many methods available to predict radiated emission have been considered. The improved partial element equivalent circuit (PEEC) method [4] is proposed to evaluate radiated emission, but it is restricted to specific models. Furthermore, the particle swarm algorithm [5], differential evolution algorithm [6] and artificial neural network [7] can predict the maximum radiated emission from printed circuit boards (PCB) by equivalent sources reconstruction based on the near-field measurement. However, their effectiveness is limited because equivalent dipoles cannot characterize the inherent structure properties of PCBs. In [8], an algorithm based on the discretization technique and the boundary integral equation is proposed to evaluate radiated emission in an IC package that are applied in the low operating frequency band.

The associate editor coordinating the review of this manuscript and approving it for publication was Giovanni Angiulli.

Additionally, in order to keep the EMI radiation below a certain level, advanced methods should also be applied to design structural parameters quickly rather than only depending on prior practical experience. Since a variety of structural parameters must be adjusted to achieve the desired properties, the problem may be posed as a multivariate structure optimization. For the optimization of structural parameters, the usual focus is to determine the next set of structural parameters in the search space by some methods, where the search space is formed by the value range of these parameters. Therefore, several stochastic optimization methods such as the genetic algorithm [9] and simulated annealing [10] can be adopted to find a solution, but these methods usually require significant computation time. Several statistical methods such as Monte Carlo analysis [11] and Bayesian optimization [12] are applied to optimize microwave circuit and device design, but large numbers of simulations are required and, with them, intractable computation.

Recently, the concept of deep learning technology has drawn considerable attention in the fields of speech recognition and image processing [13], [14]. An extensive body of studies have confirmed that deep learning models, formed by stacking multiple layers of shallow structures, have better feature representation capabilities, so nonlinear and high complexity tasks can be handled more efficiently [15]–[17]. Given the nonlinearity and complexity of current EMI issues into consideration, deep learning models could potentially be used to deal with them exactly. To our knowledge, only a few studies in this domain have considered deep learning models: modeling the high-speed channel for signal integrity analysis [18] and the prediction of high-speed via TDR impedance [19].

In this paper, a deep neural network (DNN) model is presented to accurately decipher the nonlinear black-box function between package structures and the maximum radiated electrical field at 3-meters. The trained DNN could generate sufficient data with different variance to analyze the sensitivity of structural parameters to EMI radiation. Sensitive parameters should be carefully tuned in the design process to avoid exceeding FCC requirements. As a result, the package structure can be optimized by modifying sensitive parameters and keeping others unchanged according to the correlation of structural parameters and EMI radiation.

The remaining of this paper is organized as following: Section II introduces the construction of the DNN model for EMI radiation prediction of wire-bonded ball grid array (WB-BGA) package and its flowchart. Then, the accuracy and advantages of this DNN model, as well as the hyper-parameters, are discussed in Section III. In Section IV, sensitivity analysis and the correlation of structural parameters and EMI radiation based on the trained DNN model are carried out for WB-BGA package structure optimization. In addition, the effectiveness and feasibility of the optimization method are demonstrated by the package with two sets of different structural parameters. Section V contains conclusions.

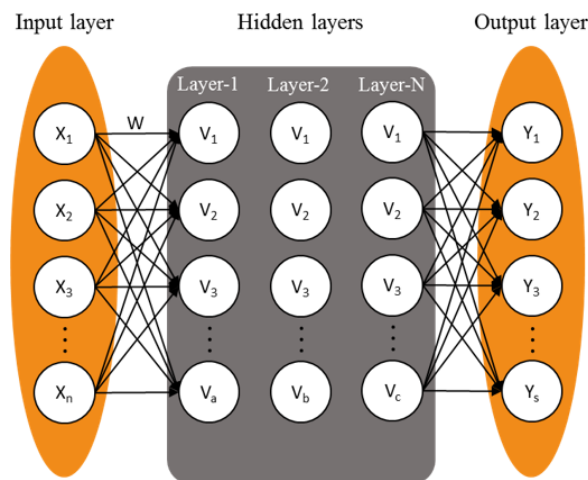


FIGURE 1. A typical, fully connected DNN model with an input layer, multiple hidden layers and an output layer.

TABLE 1. Seven key structural parameters of the WB-BGA package model.

Parameter	Description	Range
h_1	The package lid height	0.8 ~ 2.0 mm
h_2	The bump height	0.1 ~ 0.4 mm
h_3	The bonding wire height	0.21 ~ 0.33 mm
ϵ_1	The relative permittivity of the center dielectric	2 ~ 6
ϵ_2	The relative permittivity of the top and bottom dielectric	2.2 ~ 5.2
r	The signal via radius	0.05 ~ 0.2 mm
N	The number of ground vias	1 ~ 121

II. CONSTRUCTION OF DNN MODEL FOR EMI RADIATION PREDICTION OF WB-BGA PACKAGE

A DNN model consists of an input layer, multiple hidden layers and an output layer as illustrated in Fig. 1, where each layer contains multiple neurons that are fully connected to neurons of the next adjacent layer by weights. The DNN model has the capacity to learn the complex function between input features matrices and output target labels due to the multiple hidden layers and neurons.

In this study, seven key parameters of the package at the input layer are shown in Table 1, and outputs are the maximum radiated electric field at 3-meters within the 0.2 GHz to 20 GHz frequency band. Fig. 2 illustrates details of the package structure model based on the commercial WB-BGA package. Seven key design parameters with different value ranges are considered, and their description is summarized in Table 1. Symbols h_1 , h_2 , h_3 , ϵ_1 , ϵ_2 , r and N correspond to the package lid height, the bump height, the bonding wire height, the relative permittivity of the central dielectric, the relative permittivity of the top and bottom dielectric, the radius of the signal via, and the number of ground vias, respectively. The dimension of the lid and the four-layered package substrate is 26.6 mm × 26.6 mm. The die consists of

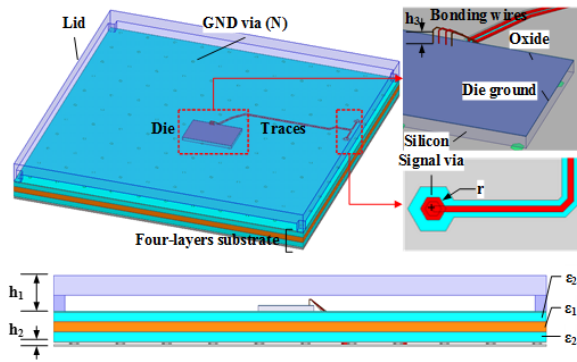


FIGURE 2. The various design parameters and structural details of the WB-BGA package model.

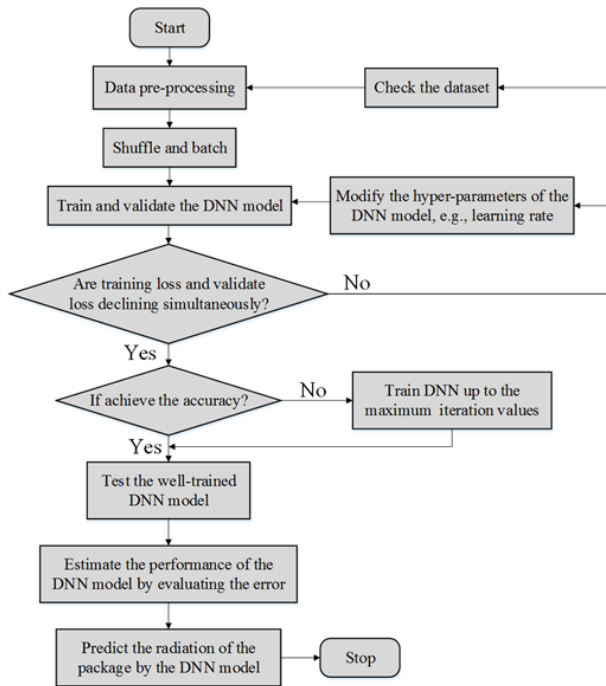


FIGURE 3. Flowchart of the DNN model for training, validation, testing and predicting.

an oxide layer, a die ground and a silicon layer, with a dimension of 4.5 mm × 4.5 mm. The 3.63 mV common-mode excitation source is located at the end of the bonding wires inside the die with the other ports terminated by 50 Ohm loads. The bonding wires are connected to differential traces with 100 Ohm differential characteristic impedance and 25 Ohm common-mode characteristic impedance, of which the length is 15 mm. The differential pair is connected to the bottom layer through signal vias and bumps.

In order to predict the EMI radiation of the WB-BGA package, the flowchart of the DNN model is given in Fig. 3, where the important process steps and issues in the DNN model development are involved as follows:

Step 1) Pre-processing the datasets: Considering features of the collected data sets have different dimensions and units,

the original data should be normalized first to ensure that these features have the same order of magnitude. Normalization of the features has the additional benefit of improving the accuracy of the DNN model and accelerating its training process. The formula of the normalization can be expressed as

$$X = (X_0 - \bar{X}) / \delta_X \quad (1)$$

where X_0 is the original value. \bar{X} is the mean value and δ_X the standard deviation of the datasets. The above normalization transforms the mean value of all features to 0 and the standard deviation of all features to 1.

Step 2) Shuffle and batch the datasets: Before training the model, normalized training datasets should be shuffled randomly to obtain good prediction performance and enhance the generalization ability of the model. Then the reshuffled datasets will be trained in batches, which have the advantages of achieving lower memory requirements and accelerating training speed.

Step 3) Train and validate the DNN model: The DNN model learns the black-box target function with training datasets, while the validation datasets are used to adjust continuously the hyper-parameters of the DNN model to attain a more accurate black-box target function. During the learning process, if the training loss and validation loss are not declining simultaneously, then both the datasets and the network structure need to be improved by cleaning the datasets and modifying the hyper-parameters of the DNN model. If the training loss and validation loss are declining simultaneously, the network is still in the process of continuous learning. When the preset accuracy is achieved, the DNN model has completed its learning process. Otherwise, continue to train and validate the DNN model up to a maximum number of iterations.

Step 4) Test the DNN model: Testing datasets are utilized to test the performance of the DNN model after learning. The root-mean-square error (RMSE), an indicator of the prediction accuracy, is adopted to evaluate the performance of the DNN model. Note that the unit of RMSE is consistent with the original data, which could be more direct to reflect the accuracy of the model than other indicators. RMSE is defined as [20]

$$RMSE = \sqrt{\frac{1}{n} \left(\sum_{i=1}^n (y_i - \hat{y}_i)^2 \right)} \quad (2)$$

where y_i is the target label data, and \hat{y}_i is the predicted data.

Step 5) Predict the EMI radiation of the WB-BGA package: The input formation for the package parameters should be consistent with the DNN input matrix. After that, the EMI radiation of the package can be obtained accurately and quickly by the trained DNN model.

III. DNN FOR RADIATION PREDICTION OF WB-BGA PACKAGE

In this study, seven hidden layers at the DNN model for EMI radiation prediction of the WB-BGA package are selected

with 300, 200, 180, 150, 120, 100 and 80 neurons at each layer, respectively. The input layer and the output layer contains 7 and 100 neurons corresponding to seven structural parameters shown in Table 1 and EMI radiation from 0.2 GHz to 20 GHz. All data are collected during the design process from full-wave simulation of the package model shown in Fig. 1. The Halton sequence is adopted to generate 2000 sets of quasi-random data of the package structures from the pre-set ranges, which are of low discrepancy and help to decrease the number of training datasets. The datasets are randomly divided into separate portions: 67.5% for training, 7.5% for validation and 25% for testing. Training datasets, validation datasets and testing datasets are independently and identically distributed.

The rectified linear unit (ReLU) function [21] is adopted as the activation function and introduce nonlinearity to the network output, which is given by

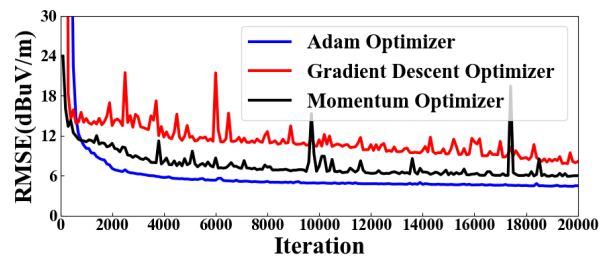
$$\text{ReLU}(v) = \max(0, v) \quad (3)$$

In addition, the batch size is set to 25. The back propagation algorithm is utilized during the development of the DNN model. The learning rate and the optimizers used in the back propagation algorithm are discussed in the following. Note that the proposed DNN model is constructed in Google's TensorFlow [22].

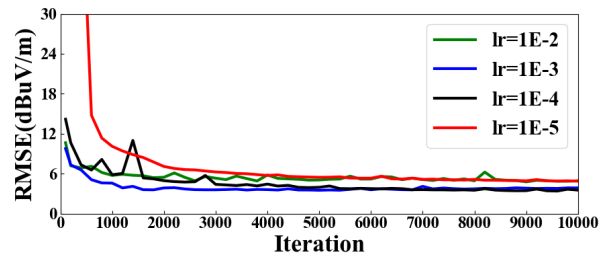
A. SELECTION OF DNN HYPER-PARAMETERS

In deep learning, different optimizers utilized in the back propagation algorithm result in different ways to search for accurate prediction results, each with different convergence rates during the training process and accuracy of the DNN model. In addition to the conventional Gradient Descent optimizer, the Momentum optimizer includes a momentum parameter that can accumulate gradient information to accelerate the learning process. The Adam optimizer combines the gradient descent algorithm and the momentum parameter and can adaptively adjust the learning rate to result in a relatively stable training process. Fig. 4 (a) shows the convergence process during the DNN model training with three different optimizers, namely the Adam optimizer, the Gradient Descent optimizer and the Momentum optimizer. Compared with the other two optimizers, the Adam optimizer is demonstrated to have faster and more stable convergence in the training process, which also illustrates the best accuracy in this work.

Furthermore, the learning rate is another important parameter of the DNN model. It is step-size taken at each iteration, which controls the learning progress of the model. If the learning rate is small, the training process will converge slowly and increase the training time. In addition, a small learning rate may also cause over-fitting, which means the DNN model will only remember the datasets rather than learn the implicit function between the structural parameters and the EMI radiation. Conversely, if the learning rate is large, although the training process will be fast, it may cause non-convergence and under-fitting of the model, which means the DNN model will not capture the implicit input to output



(a) RMSE vs. iteration for three different optimizers



(b) RMSE vs. iteration for four different values of the learning rate

FIGURE 4. Evolution of the RMSE during the learning process of the DNN model for EMI radiation prediction of WB-BGA package.

function. Consequently, there exists an application dependent trade-off for the learning rate. Fig. 4 (b) illustrates the training process with different values of the learning rate in this DNN model with the Adam optimizer. When the learning rate is 10^{-3} , the accuracy of the model is best and the model does not exhibit under-fitting or over-fitting according to the Step 3) in Fig. 3. The learning process with a 10^{-3} learning rate is more stable than others as well as acceptable training speed. Therefore, the value of 10^{-3} is chosen as the optimal learning rate in this work.

B. PERFORMANCE AND RESULTS

Four representative sets of data from test datasets are chosen discretionarily to illustrate the deviation of the predicted EMI radiation and target labeled radiation of the WB-BGA package. Predicted results are calculated from the DNN model, and the target labeled results are from full-wave simulation. Fig. 5 shows the comparison of predicted results and the corresponding labeled results based on the four cases. The radiation predicted by the proposed DNN model has good agreement with the target labeled radiation. Fig. 6 shows the average relative error of predicted results based on all test data. The relative error at every frequency is all below 2%, which proves the trained DNN model fits well for this work.

Additionally, the RMSE for the test data is 1.87 dBuV/m and the RMSE for the validation data is 1.91 dBuV/m when predicting the EMI radiation of the WB-BGA package. Once the DNN model is developed, the computing time for one prediction run of the developed DNN model is on the order of milliseconds. In addition, the model size is only 3 MB that can greatly save storage space when repeatedly computing EMI radiation. As a result, the trained DNN model for EMI

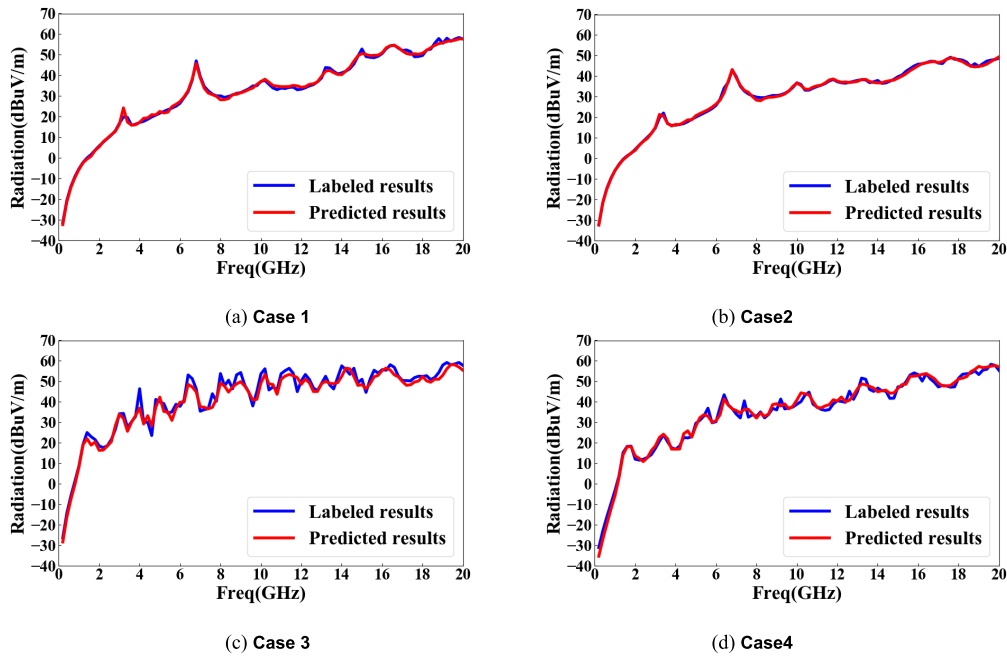


FIGURE 5. The comparison of the predicted results and the labeled results in four cases. (a) Case 1 with structural parameters ($h_1, h_2, h_3, \epsilon_1, \epsilon_2, r, N$) in sequence of (0.89, 0.31, 0.32, 2.41, 4.60, 0.18, 76), (b) Case 2 with structural parameters (1.28, 0.38, 0.28, 3.48, 3.42, 0.12, 103), (c) Case 3 with structural parameter (1.21, 0.19, 0.23, 5.45, 5.08, 0.08, 16), and (d) Case 4 with structural parameters (1.52, 0.14, 0.25, 4.74, 4.55, 0.18, 23). Predicted results are from DNN model, and labeled results are from full-wave simulation.

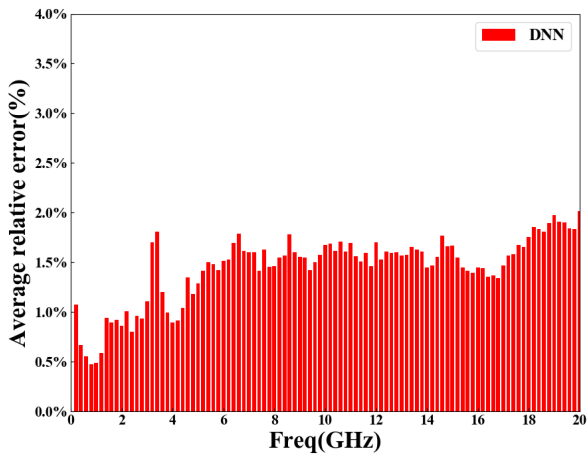


FIGURE 6. The average relative error of the DNN model over the complete frequency band of the test datasets.

radiation prediction of the WB-BGA package has the advantages of low computation cost and small memory usage while also achieving good accuracy.

IV. DNN FOR WB-BGA PACKAGE STRUCTURE OPTIMIZATION

The WB-BGA package EMI radiation must satisfy the EMI design as well as performance requirements, where the maximum radiated electric field at 3-meters from the package cannot exceed 54 dBuV/m (FCC requirement) within the two frequency ranges of 9 GHz to 11 GHz and 18 GHz to 20 GHz. The former requirement is because the operating frequency of the package and chip is at 10 GHz and the latter one is because

the operating frequency of the package could be higher in future designs. These two aims are taken into consideration for sensitivity analysis and structure optimization of the WB-BGA package.

A. SENSITIVITY ANALYSIS OF PACKAGE STRUCTURES

In order to evaluate the sensitivity of the seven design parameters of WB-BGA packages to EMI radiation, each parameter should be discussed separately. For example, the discreteness of h_1 should be adjusted while others remain the same when analyzing the sensitivity of h_1 . Meanwhile, the mean of all parameters remains unchanged. The standard deviation is adopted to measure datasets discreteness. Finally, the sensitivity can be quantified by the pass rate, which is expressed as

$$pass_rate = \frac{num_p}{num_{tot}} \tag{4}$$

where num_p is the number of structures that satisfy the radiation requirements in the two frequency ranges, and num_{tot} is the total number of structures.

Table 2 tabulates the pass rate for the seven design parameters and different discreteness. The lid height h_1 is chosen as one design parameter due to the practical assembly error. The bump height h_2 and the number of ground vias N are analyzed because package structures tend to be miniaturized in the future so it is important to reduce the real estate consumed by the ground vias N when satisfying the EMI requirement. Ground vias are connected to the bumps, hence the bump height may cause EMI risk. Besides, the bonding wire height h_3 and the signal vias radius r could lead to

TABLE 2. The pass rate of the WB-BGA package structural parameters subject to different values of standard deviation.

Parameter	Pass Rate			
	sd_0	$sd_3=sd_0*3$	$sd_5=sd_0*5$	$sd_{10}=sd_0*10$
h_1 (mean = 1.4) (sd = 0.05)	96.35%	96.10%	95.51%	96.98%
h_2 (mean = 0.25) (sd = 0.014)	96.35%	96.45%	96.51%	96.88%
h_3 (mean = 0.27) (sd = 0.006)	96.35%	96.13%	95.37%	93.88%
ε_1 (mean = 4) (sd = 0.2)	96.35%	96.05%	95.14%	94.48%
ε_2 (mean = 3.7) (sd = 0.15)	96.35%	82.16%	52.12%	51.23%
r (mean = 0.125) (sd = 0.006)	96.35%	89.99%	78.56%	55.57%
N (mean = 61) (sd = 4)	96.35%	95.13%	92.33%	68.37%

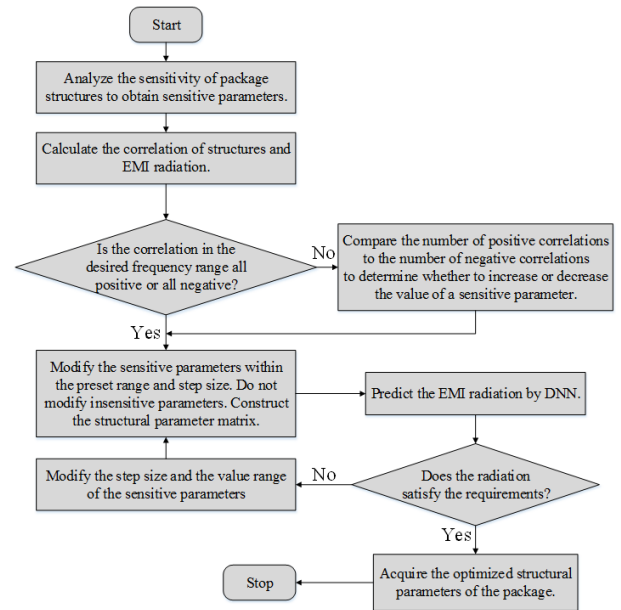
(sd denotes standard deviation. sd_0 is the original standard deviation of each parameter, and sd_3 , sd_5 , and sd_{10} are 3 times, 5 times, and 10 times of the original standard deviation.)

unintentional radiation. The permittivity of the dielectric ε_1 and ε_2 are taken into account due to the package cost.

As shown in Table 2, the datasets with 3, 5 and 10 times standard deviation are generated by the well-trained DNN model in Section III, and the total number of these datasets is 20000. The parameters h_1 , h_2 , h_3 and ε_1 can maintain a good pass rate even when the standard deviation is changed from 1 to 10 times. The pass rate of ε_2 is below 85% when the standard deviation is 3 times of the original. It drops to about 50% when the standard deviation is increased to 5 and 10 times. The trend implies that ε_2 is very sensitive to the EMI radiation. In addition, r and N are also sensitive when the standard deviation is 5 times and 10 times, so they should be appropriately and carefully considered in the package design process to achieve better EMI performance. Thus, this tabulation can quantify the sensitivity of each key parameter to EMI radiation and provides insightful guidance for the design of package structures.

B. OPTIMIZATION METHOD

According to the results in Table 2, among all the 7 key parameters, the permittivity of the top and bottom dielectric ε_2 , the signal vias radius r and the number of ground vias N are the three critical parameters most sensitive to the EMI radiation. For a WB-BGA package with severe unintentional radiation, the structure parameters can be rapidly optimized to satisfy the EMI design and performance requirements by modifying sensitive parameters. Fig. 7 illustrates the flowchart for WB-BGA package structure optimization with key process steps detailed as follows:

**FIGURE 7.** Flowchart of the WB-BGA package structural optimization based on sensitivity analysis and correlations.

Step 1) Sensitivity analysis: The sensitive parameters can be obtained by the analysis of Table 2 in Section IV.

Step 2) Calculate the correlation between structures and EMI radiation: The next set of structural parameters is to be acquired by modifying the sensitive parameters ε_2 , r and N while keeping others (i.e., h_1 , h_2 , h_3 and ε_1) unchanged. The correlations of structures and EMI radiation at each frequency are calculated to determine how to adjust the sensitive parameters. Since small changes of sensitive parameters could cause dramatic changes to EMI radiation, the trends of radiation while adjusting structure parameters are more important than whether their correlations are linear or nonlinear. As a result, the Pearson correlation coefficient [20] is adopted and can be expressed as

$$\rho_{X,Y} = \frac{\text{cov}(X, Y)}{\sigma_X \sigma_Y} \quad (5)$$

where $\text{cov}(X, Y)$, σ_X and σ_Y are the covariance and the standard deviation of variables X and Y . If the positive and negative correlations are consistent in the desired frequency range, the sensitive parameters ε_2 , r and N will be modified according to the preset step and value range. Otherwise, it is important to check the magnitude of the correlation coefficient ($|\rho|$). When $|\rho|$ is larger than 0.3, the structural parameters and the EMI radiation have a strong correlation. If the number of strong positive correlations in a desired frequency range is more than the number of negative correlations, the sensitive parameters should be modified depending on the positive correlations. By now the next structural parameters matrix is completely constructed.

Step 3) Predict the EMI radiation: The radiation of a WB-BGA package can be predicted quickly and accurately by the well-trained DNN model as shown in Section II when

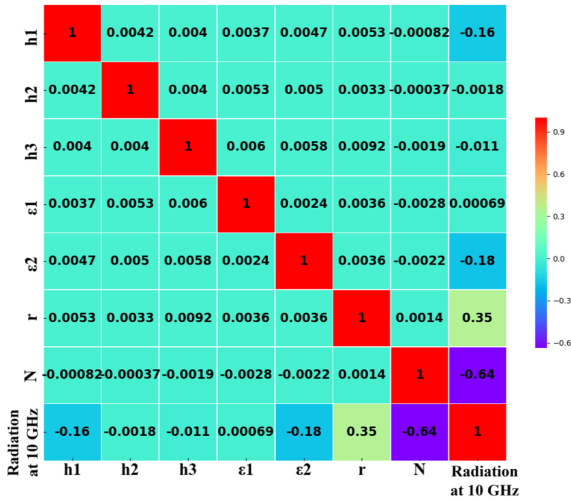


FIGURE 8. The heat map of the correlations of the package structures and the EMI radiation at 10 GHz.

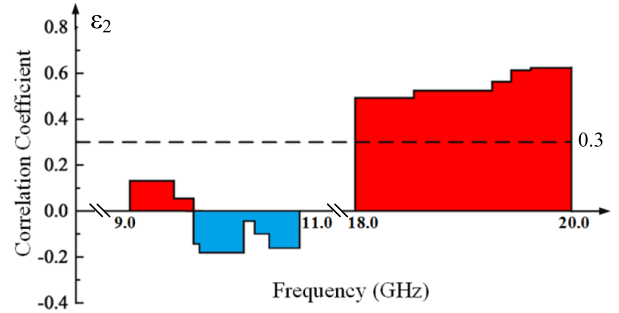
inputting the matrix of package structures determined in Step 2).

Step 4) Acquire the optimized structural parameters: If the predicted radiation in Step 3) satisfies the EMI performance requirement, the corresponding structural parameters are the optimized results. Otherwise, Step 2) is repeated to adjust the value range of the sensitive parameters as well as the step size. Generally, a small value range and large step size works well to quickly optimize the package structure. For extremely sensitive parameters, the step size should be further decreased because the EMI radiation could change drastically even with a small change in these parameters.

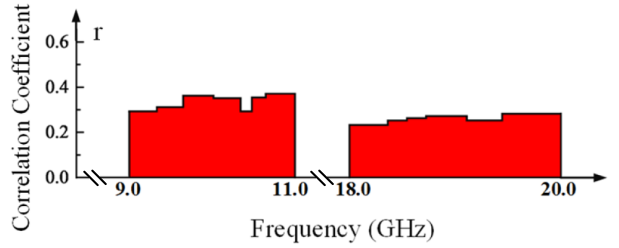
C. EXAMPLES AND RESULTS

In this work, the WB-BGA package with two sets of different structural parameters are used as numerical cases to verify the proposed optimization method to avoid EMI radiation exceeding 54 dBuV/m within the two frequency ranges: 9 GHz to 11 GHz and 18 GHz to 20 GHz.

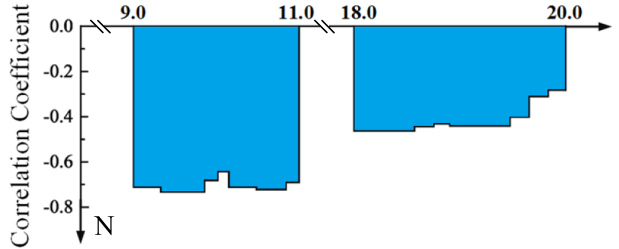
To begin, the sensitive parameters of this WB-BGA package structure are identified as ϵ_2 , r and N through the analysis in Table 2. Then, the correlations of seven structural parameters and the EMI radiation at each frequency (e.g., 10 GHz) are quantified by the Pearson correlation coefficient (cf. Eq. (5)) as illustrated in Fig. 8. Its last row or column shows that the correlation coefficients between the sensitive parameters (i.e., ϵ_2 , r and N) and radiation at 10 GHz are -0.18 , 0.35 and -0.64 , respectively. In this way, the correlation coefficient distribution of the sensitive parameters and the EMI radiation from 9 GHz to 11 GHz and from 18 GHz to 20 GHz can be collected, which are shown in Fig. 9. In this work, r is positively related and N is negatively related to the EMI radiation in the desired frequency range, so r should be decreased and N should be increased to satisfy the EMI requirement when constructing the structural parameter matrix at each iteration. However, the positive and negative correlation of ϵ_2 is not consistent in the frequency



(a) The correlation coefficient distribution for parameter ϵ_2



(b) The correlation coefficient distribution for parameter r



(c) The correlation coefficient distribution for parameter N

FIGURE 9. The correlation coefficient distribution of the sensitive parameters and the EMI radiation within the frequency range from 9 GHz to 11 GHz and from 18 GHz to 20 GHz. (a) The permittivity of the top and bottom dielectric ϵ_2 , (b) the signal via radius r , and (c) the number of ground vias N .

range under consideration. As shown in Fig. 9 (a), it is obvious that the number of strong positive correlations ($|\rho| > 0.3$) is more than the number of negative correlations in the two frequency range. Consequently, ϵ_2 should be decreased for EMI radiation mitigation.

Furthermore, the value ranges of the sensitive parameters are same as those in Table 1. Since ϵ_2 is more sensitive to the EMI radiation than r and N , a smaller step size of ϵ_2 should be chosen while a larger step size can be used for other sensitive parameters. The actual values of the step size for ϵ_2 , r and N used in this work are 0.02, 0.03 and 6, respectively.

Finally, Fig. 10 is presented to compare the radiation before and after the optimization of two sets of different structural parameters. After optimization, the maximum electric field at 3-meters for both cases do not exceed 54 dBuV/m within the frequency range from 9 GHz to 11 GHz and from 18 GHz to 20 GHz. The optimized structural parameters are shown in Table 3. As a result, the structure optimization method based on the DNN model is demonstrated to have good effectiveness.

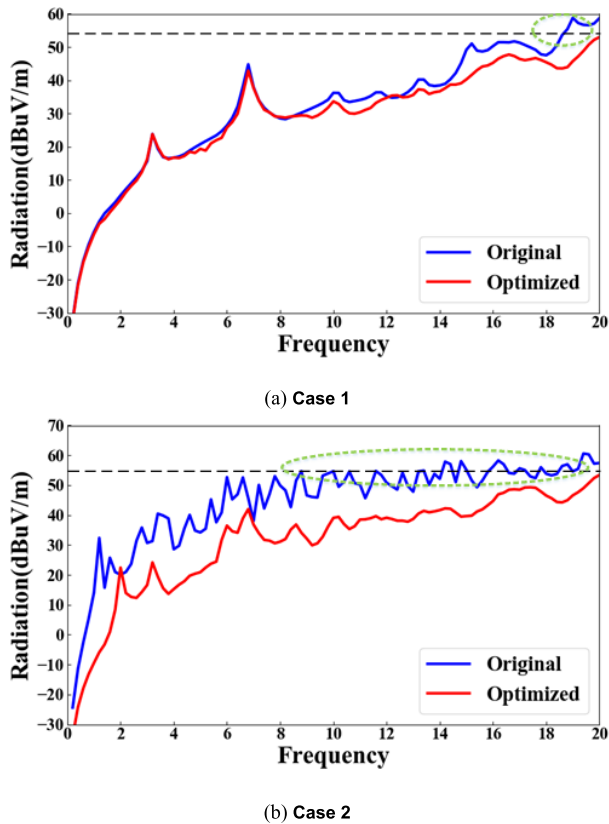


FIGURE 10. Comparison of the optimized results based on the proposed optimization method with the original results prior to optimization.

TABLE 3. The structural parameters of the WB-BGA package before and after optimization.

Parameter	Example 1		Example 2	
	Before	After	Before	After
h_1	1.13	1.13	0.94	0.94
h_2	0.31	0.31	0.33	0.33
h_3	0.25	0.25	0.29	0.29
ε_1	5.22	5.22	4.65	4.65
ε_2	4.42	4.04	4.92	4
r	0.14	0.05	0.19	0.07
N	121	121	9	45

V. CONCLUSION

In this paper, a DNN model is employed to predict EMI radiation for a realistic commercial WB-BGA package. The DNN model with 10^{-3} learning rate and Adam optimizer can lead to rapid and stable convergence, and achieve good accuracy where the RMSE is 1.87 dBuV/m and the average relative error is below 2%. The computing time for running one EMI prediction is on the order of milliseconds once the DNN model is developed. Taking advantage of the trained DNN model, the sensitivity of seven structural parameters is able to be quantified by the pass rate. The three parameters ε_2 , r and N are found to be sensitive to the EMI radiation in this work, where ε_2 is the most sensitive one. The sensitive parameter analysis together with their correlations facilitates

the construction of an updated set of structural parameters in the optimization process, which resolves a key and difficult step for structural optimization. Finally, the WB-BGA package structure was optimized to satisfy the EMI performance requirement that the maximum electric field at 3-meters cannot exceed 54 dBuV/m in the frequency range from 9 GHz to 11 GHz and 18 GHz to 20 GHz. Two numerical cases of a WB-BGA package with different structural parameters are conducted, which verifies and demonstrates the effectiveness of the proposed optimization method.

REFERENCES

- [1] T. Sudo, H. Sasaki, N. Masuda, and J. L. Drewniak, "Electromagnetic interference (EMI) of system-on-package (SOP)," *IEEE Trans. Adv. Packag.*, vol. 27, no. 2, pp. 304–314, May 2004.
- [2] C.-Y. Hsiao, C.-H. Cheng, and T.-L. Wu, "A new broadband common-mode noise absorption circuit for high-speed differential digital systems," *IEEE Trans. Microw. Theory Techn.*, vol. 63, no. 6, pp. 1894–1901, Jun. 2015.
- [3] X.-L. Yang, L. Zhang, Y.-S. Li, H. Jin, P. Cheng, Y. Li, and E.-P. Li, "A novel package lid using mushroom-type ebg structures for unintentional radiation mitigation," *IEEE Trans. Electromagn. Compat.*, vol. 60, no. 6, pp. 1882–1888, Dec. 2018.
- [4] Y.-A. Hsu, C.-C. Chou, C.-H. Cheng, and T.-L. Wu, "A radiation prediction method based on partial element equivalent circuit," in *Proc. Asia-Pacific Electromagn. Compat. Symp.*, Shenzhen, China, Jul. 2016, pp. 706–708.
- [5] F.-P. Xiang, E.-P. Li, X.-C. Wei, and J.-M. Jin, "A particle swarm optimization-based approach for predicting maximum radiated emission from PCBs with dominant radiators," *IEEE Trans. Electromagn. Compat.*, vol. 57, no. 5, pp. 1197–1205, Oct. 2015.
- [6] W.-J. Zhao, B.-F. Wang, E.-X. Liu, H. B. Park, H. H. Park, E.-P. Li, and E. Song, "An effective and efficient approach for radiated emission prediction based on amplitude-only near-field measurements," *IEEE Trans. Electromagn. Compat.*, vol. 54, no. 5, pp. 1186–1189, Oct. 2012.
- [7] S. Yao, Y. F. Shu, L. Tong, X. C. Wei, Y. B. Yang, and E. X. Liu, "An equivalent radiation source based on artificial neural network for EMI prediction," in *Proc. IEEE Int. Symp. Electromagn. Compat. (EMC EUROPE)*, Amsterdam, The Netherlands, Aug. 2018, pp. 556–560.
- [8] S. Wen, J. Zhang, and Y. Lu, "Modeling and quantification for electromagnetic radiation of power-bus structure with multilayer printed circuit board," *IEEE Trans. Compon., Packag., Manuf. Technol.*, vol. 6, no. 1, pp. 79–86, Jan. 2016.
- [9] Y. A. Hussein and S. M. El-Ghazaly, "Modeling and optimization of microwave devices and circuits using genetic algorithms," *IEEE Trans. Microw. Theory Techn.*, vol. 52, no. 1, pp. 329–336, Jan. 2004.
- [10] L. Zuo, L. Shu, S. Dong, C. Zhu, and T. Hara, "A multi-objective optimization scheduling method based on the ant colony algorithm in cloud computing," *IEEE Access*, vol. 3, pp. 2687–2699, 2015.
- [11] J. E. Rayas-Sánchez and V. Gutiérrez-Ayala, "EM-based Monte Carlo analysis and yield prediction of microwave circuits using linear-input neural-output space mapping," *IEEE Trans. Microw. Theory Techn.*, vol. 54, no. 12, pp. 4528–4537, Dec. 2006.
- [12] P. Chen, B. M. Merrick, and T. J. Brazil, "Bayesian optimization for broadband high-efficiency power amplifier designs," *IEEE Trans. Microw. Theory Techn.*, vol. 63, no. 12, pp. 4263–4272, Dec. 2015.
- [13] D. Wang and J. Chen, "Supervised speech separation based on deep learning: An overview," *IEEE/ACM Trans. Audio, Speech, Language Process.*, vol. 20, no. 10, pp. 1702–1726, Oct. 2018.
- [14] D. Hu, S. Zhou, Q. Shen, S. Zheng, Z. Zhao, and Y. Fan, "Digital image steganalysis based on visual attention and deep reinforcement learning," *IEEE Access*, vol. 7, pp. 25924–25935, 2019.
- [15] Y. LeCun, Y. Bengio, and G. Hinton, "Deep learning," *Nature*, vol. 521, pp. 436–444, May 2015.
- [16] P. Vincent, H. Larochelle, I. Lajoie, Y. Bengio, and P.-A. Manzagol, "Stacked denoising autoencoders: Learning useful representations in a deep network with a local denoising criterion," *J. Mach. Learn. Res.*, vol. 11, no. 12, pp. 3371–3408, Dec. 2010.
- [17] S.-H. Fang, Y.-X. Fei, Z. Xu, and Y. Tsao, "Learning transportation modes from smartphone sensors based on deep neural network," *IEEE Sensors J.*, vol. 17, no. 18, pp. 6111–6118, Sep. 2017.

- [18] T. Lu, J. Sun, K. Wu, and Z. Yang, "High-speed channel modeling with machine learning methods for signal integrity analysis," *IEEE Trans. Electromagn. Compat.*, vol. 60, no. 6, pp. 1957–1964, Dec. 2018.
- [19] J. Xu, L. Zhang, M. Sapozhnikov, and J. Fan, "Application of deep learning for high-speed differential via TDR impedance fast prediction," in *Proc. IEEE Symp. Electromagn. Compat., Signal Integr. Power Integr. (EMC, SI PI)*, Long Beach, CA, USA, Jul./Aug. 2018, pp. 645–649.
- [20] R. Larson and B. Farber, *Elementary Statistics: Picturing the World*. London, U.K.: Pearson, 2011.
- [21] V. Nair and G. E. Hinton, "Rectified linear units improve restricted Boltzmann machines," in *Proc. Int. Conf. Mach. Learn.*, 2010, pp. 807–814.
- [22] M. Abadi et al., "TensorFlow: Large-scale machine learning on heterogeneous distributed systems," 2016, *arXiv:1603.04467*. [Online]. Available: <https://arxiv.org/abs/1603.04467>



HANG JIN received the B.S. degree in electronic science and technology from the Huazhong University of Science and Technology, Wuhan, China, in 2016. He is currently pursuing the Ph.D. degree in electronic science and technology with Zhejiang University, Hangzhou, China.

His research interest includes machine learning for complex EMI issues, EMI source localization, and EMI issues of systems in package.



HANZHI MA received the B.S. degree in engineering from Zhejiang University, Hangzhou, China, in 2017. She is currently pursuing the Ph.D. degree with the Department of IS and Electronic Engineering, Zhejiang University–University of Illinois at Urbana–Champaign Institute, Zhejiang University.

Her current research interest includes machine learning technique for EMI/SI/PI analysis.



MARK D. BUTALA received the H.B.E.E. degree in electrical engineering from the University of Delaware, Newark, DE, USA, in 2002, and the M.S. and Ph.D. degrees in electrical and computer engineering from the University of Illinois Urbana–Champaign (UIUC), IL, USA, in 2004 and 2010, respectively.

From 2010 to 2015, he was a Member of the Technical Staff with the Jet Propulsion Laboratory, California Institute of Technology, Pasadena, CA, USA, as a member of the ionospheric and atmospheric remote sensing group working primarily on global navigation satellite system based specification of the global ionosphere. From 2016 to 2017, he was a Visiting Research Scientist with the Department of Electrical and Computer Engineering, UIUC, where he studied power transmission system impacts of geomagnetically induced currents. Since 2017, he has been with the Faculty of Zhejiang University, Hangzhou, Zhejiang, China, where he is currently an Assistant Professor with College of Information Science and Electronics Engineering, Zhejiang University–University of Illinois at Urbana–Champaign Institute, and also an Adjunct Assistant Professor with the Department of Electrical and Computer Engineering, UIUC. His research interests include remote sensing, image reconstruction and tomography, statistical signal, and image processing theory and application.

Dr. Butala received a National Science Foundation Graduate Research Fellowship, in 2002, a UIUC Department of Electrical and Computer Engineering Distinguished Fellowship, in 2005, a UIUC Computational Science and Engineering Fellowship, in 2008, and a Massachusetts Institute of Technology Lincoln Laboratories Graduate Fellowship, in 2008. He was a recipient of three NASA Group Achievement Awards.



EN-XIAO LIU (M'05–SM'09) received the Ph.D. degree in electrical engineering from the National University of Singapore (NUS), in 2005.

From 1999 to 2001, he was with the North China Electric Power Design Institute, Beijing, China. In 2005, he joined the Institute of High Performance Computing (IHPC), Agency for Science Technology and Research (A*STAR), Singapore, where he is currently a Senior Scientist and the Deputy Department Director of the Electronics and Photonics Department. He is also an Adjunct Associate Professor with the Electrical and Computer Engineering Department, NUS. He has published more than 100 papers and three book chapters. His research interests include computational electromagnetics, high-speed electronics, and electromagnetic compatibility (EMC).

Dr. Liu received the Borderless Silver Award of the Singapore Ministry of Trade Industry (MTI), in 2015, the Technical Achievement Award from the IEEE EMC Society, in 2016, the Prestigious Engineering Achievement Award of Institution of Engineers Singapore (IES), in 2019, and several Best Paper and Best Industry Project Awards. He was an IEEE EMC Society Distinguished Lecturer. He has been serving the IEEE EMC Singapore Chapter in different roles such as a Chair and an Executive Committee Member, and contributing regularly to various international conferences in different capacities, such as an Organizing Chair, a Technical (Program) Chair, an International Advisory or Steering Committee Member, and a General Chair. He is currently an Associate Editor of two IEEE Transactions journals.



ER-PING LI (S'91–M'92–SM'01–F'08) has served as a Research Fellow, a Principal Research Engineer, an Associate Professor, and the Technical Director for the Singapore Research Institute and University, since 1989. In 2000, he joined the Singapore A*STAR Research Institute of High Performance Computing as a Principal Scientist and the Director. He is currently a Changjiang–Qianren Distinguished Professor with the Department of Information Science and

Electronic Engineering, Zhejiang University, China; the Dean of the Joint Institute, Zhejiang University–University of Illinois at Urbana–Champaign Institute. He authored or coauthored more than 500 papers published in the referred international journals and conferences, authored two books published by John–Wiley–IEEE Press and Cambridge University Press. He holds and has filed a number of patents at the U.S. patent office. His research interests include electrical modeling and design of micro/nano-scale integrated circuits, 3D electronic package integration, and nano-plasmonic technology.

Dr. Li is a Fellow of MIT Electromagnetics Academy, USA. He is the Founding Member of IEEE MTT-RF Nanotechnology Committee. He was a recipient of the 2015 IEEE Richard Stoddard Award on EMC, the IEEE EMC Technical Achievement Award, the Singapore IES Prestigious Engineering Achievement Award, and the Changjiang Chair Professorship Award from the Ministry of Education in China, and number of Best Paper Awards. He has been a General Chair and a Technical Chair for many international conferences. He was the Founding General Chair for Asia-Pacific EMC Symposium, the General Chair for 2008, 2010, 2012, 2016 APEMC, and the 2010 IEEE Symposium on Electrical Design for Advanced Packaging Systems. He served as an Associate Editor for the IEEE *Microwave and Wireless Components Letters* from 2006 to 2008 and served as a Guest Editor for 2006 and 2010 IEEE Transactions on EMC Special Issues, a Guest Editor for the 2010 IEEE TRANSACTIONS ON MTT APMC Special Issue. He is currently an Associate Editor for the IEEE TRANSACTIONS ON EMC and the IEEE TRANSACTIONS ON CPMT. He has been invited to give numerous invited talks and plenary speeches at various international conferences and forums. He was elected to the IEEE EMC Distinguished Lecturer, in 2007. He was the President of the 2006 International Zurich Symposium on EMC.

• • •